



A magnetic nanomaterial modified with poly-lysine for efficient removal of anionic dyes from water



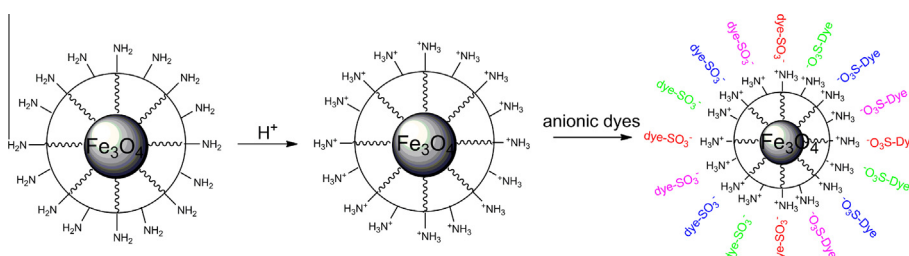
Yan-Ru Zhang, Peng Su, Jun Huang, Qing-Rong Wang, Bao-Xiang Zhao*

Institute of Organic Chemistry, School of Chemistry and Chemical Engineering, Shandong University, Jinan 250100, PR China

HIGHLIGHTS

- The adsorbent can be conveniently separated and effectively reused.
- The surface containing lots of amino groups can enhance the adsorption capacities for anionic dyes.
- Low toxic organosilane and poly-lysine were used as raw materials.

GRAPHICAL ABSTRACT



ARTICLE INFO

Article history:

Received 7 August 2014

Received in revised form 26 September 2014

Accepted 27 September 2014

Available online 5 October 2014

Keywords:

Magnetic nanoparticles
Poly-lysine
Adsorption
Anionic dyes

ABSTRACT

This work describes the synthesis and adsorption behavior of Fe_3O_4 magnetic nanoparticles (MNPs) modified with 3-glycidoxypropyltrimethoxysilane (GPTMS) and poly-lysine (P-Lys). The magnetic nanoparticles were characterized by infra-red spectra, transmission electron microscopy, X-ray diffraction, thermogravimetric analysis and X-ray photoelectron spectroscopy. To understand the adsorption mechanism of the MNPs, we investigated anionic dye uptake capacity of Fe_3O_4 @GPTMS@P-Lys as a function of contact time, dye concentration and pH. The MNPs could effectively remove anionic dyes including methyl blue (MB), orange I (OR-I), amaranth (AM) and acid red 18 (AR-18) from water solution. Furthermore, the improved adsorbent showed convenient separation and efficient reusability, and enhanced the adsorption capacity for anionic dyes.

© 2014 Elsevier B.V. All rights reserved.

1. Introduction

Dye is one of the most significant identified contaminant among the various pollutants of wastewater because of its high toxicity and possible accumulation in the environment. At the same time, organic dyes are extensively used in various branches such as textile, paper, printing, color photography, pharmaceutical, leather, cosmetics, plastic and other industries [1]. Many of these dyes are carcinogenic, mutagenic and teratogenic, so they are toxic to human, microorganisms and fish species. Removal of dyes from wastewater becomes environmentally important [2]. So far, several technologies, including adsorption, coagulation,

flocculation, advanced oxidation processes, ozonation, membrane filtration and biological treatment, have been developed and implemented for the purpose of removing the dyes from wastewater [3,4]. Adsorption is an attractive method for the removal of organic dye because of its low cost [5]. Therefore, many adsorbents such as activated carbon [6], kaolin [7], montmorillonite clay [8], waste red mud [9], fullers earth and fired clay [10], were reported to decolorize wastewater. As adsorbent, magnetic nanomaterial possessing large surface areas, unique magnetic properties and low cost, has become an increasingly popular tool in various fields. Because Fe_3O_4 nanoparticles are biocompatible, low toxic, easily synthesized, particularly economic and environmental friendly [11], many adsorbents were synthesized through surface modification of Fe_3O_4 nanoparticles with diverse organic compounds. However, a few papers have reported on

* Corresponding author. Tel.: +86 531 88366425; fax: +86 531 88564464.

E-mail address: bxzhao@sdu.edu.cn (B.-X. Zhao).

the adsorption of dyes by the magnetic particles cross-linked with amino acid until now.

In our previous work, we reported four kinds of magnetic adsorbents for removing organic dyes [12–15]. The magnetic adsorbent modified with lysine ($\text{Fe}_3\text{O}_4\text{@GPTMS@Lys}$) could remove cationic and anionic dyes. However, the maximum adsorption quantity (q_m) for anionic dye is below 100 mg/g [15]. In this work, Fe_3O_4 nanoparticles modified with poly-lysine ($\text{Fe}_3\text{O}_4\text{@GPTMS@P-Lys}$) could enhance the maximum adsorption capacity for various anionic dyes including methyl blue (MB), orange I (OR-I), amaranth (AM) and acid red 18 (AR-18) (Fig. 1), because the number of amino group influences q_m for anionic dyes and poly-lysine contains much more amino groups than lysine. We have studied the adsorption isotherms, kinetics, desorption and reuse of the MNPs. Furthermore, the $\text{Fe}_3\text{O}_4\text{@GPTMS@P-Lys}$ MNPs possess high surface areas which lead to higher adsorption capacity and strong superparamagnetic properties that can be handled in an external magnetic field [16].

2. Experimental

2.1. Apparatus and reagents

All reagents were of analytical reagent-grade and were used as supplied. Ferric chloride ($\text{FeCl}_3 \cdot 6\text{H}_2\text{O}$), ferrous sulfate ($\text{FeSO}_4 \cdot 7\text{H}_2\text{O}$), poly-lysine, anhydrous sodium carbonate (Na_2CO_3) and four organic dyes acid red 18 (AR-18), orange I (OR-I), methyl blue (MB), amaranth (AM) were purchased from Sinopharm Chemical. Sodium hydroxide (NaOH) and toluene were from Tianjin Guangcheng Chemical. 3-Glycidoxypropyltrimethoxysilane (GPTMS) was from J&K Chemical. Aqueous solutions of organic dyes were prepared with deionized water.

2.2. Characterization

The particle size and morphological characteristics of the MNPs were detected with a transmission electron microscope (TEM, JEM-1011). Infra-red (IR) spectra were recorded with an IR spectrophotometer Bruker VERTEX 70 FT-IR (Germany). The magnetic properties of the MNPs were analyzed by a vibrating sample magnetometer (VSM, JDM-13E). Thermo gravimetric analysis (TGA) involved use of an SDTQ600 thermo gravimetric analyzer (USA) at 10 °C/min under nitrogen flow. A Bruker D8 Advance X-ray diffraction analyzer (Germany) with Cu K α radiation was used for X-ray diffraction (XRD) measurements. pH values were measured with a PHS-3C pH-meter (Tianyou, Shanghai). A UV-4100 spectro-

photometer (Hitachi) was used to determine organic dyes concentration in solution. Zeta potential of synthesized materials was measured with Zeta PALS (USA). The specific surface area and pore size distribution were performed with Surface Area and Porosity Analyzer (ASAP 2020 HD88). X-ray photoelectron spectroscopy (XPS) was recorded on ESCALAB 250 (ThermoFisher SCIENTIFIC).

2.3. Preparation of magnetic nanoparticles

Fe_3O_4 nanoparticles were prepared by a chemical coprecipitation method [17]. Briefly, a solution (50 mL) of mixture of $\text{FeSO}_4 \cdot 7\text{H}_2\text{O}$ (0.01 M) and $\text{FeCl}_3 \cdot 6\text{H}_2\text{O}$ (0.02 M) (molar ratio 1:2) was added dropwise into 250 mL of alkali solution (0.75 M NaOH) in deionized water (deoxygenated before use) under nitrogen gas protection and vigorous stirring using nonmagnetic stirrer for 30 min at 80 °C. After the reaction, the Fe_3O_4 precipitate was obtained by magnetic separation and washed with 200 mL deionized water (deoxygenated before use) 3 times, 150 mL anhydrous ethanol 3 times. The precipitate was dried under vacuum [18,19].

The $\text{Fe}_3\text{O}_4\text{@GPTMS}$ MNPs were synthesized according to the previous reported methods [14,15,20]. 1.00 g Fe_3O_4 MNPs were suspended in 100 mL distilled toluene by ultrasonicator for 10 min. The dispersion was heated to reflux with vigorous stirring under nitrogen gas, and then 8 mL GPTMS was added. The mixture was kept refluxing for 8 h. The obtained products were separated from magnetic field and washed three times with deionized water and anhydrous ethanol, finally, dried at 60 °C under vacuum for 3 h (Scheme S1, ESI).

The $\text{Fe}_3\text{O}_4\text{@GPTMS@P-Lys}$ MNPs were synthesized from $\text{Fe}_3\text{O}_4\text{@GPTMS}$ and poly-lysine as described with some modifications [21]. Typically, $\text{Fe}_3\text{O}_4\text{@GPTMS}$ MNPs (2.605 g), poly-lysine (2.0 g), sodium carbonate (2.605 g) and deionized water (50 mL) were added into a round-bottomed flask under mechanical agitation and nitrogen gas protection. The mixture was stirred for 24 h at room temperature. Subsequently, the obtained product was separated by a magnet. After immergence of the precipitate in dilute acetic acid for 10 min, the precipitate was washed several times with deionized water and anhydrous ethanol. The final product was dried in a vacuum system at 60 °C for 8 h.

2.4. Adsorption experiments

All adsorption experiments were executed on a model SHA-B thermostat shaker (Changzhou, China) with a shaking speed of 300 rpm. Briefly, 50 mg adsorbents ($\text{Fe}_3\text{O}_4\text{@GPTMS@P-Lys}$ MNPs) were added into 50 mL organic dyes solution of known concentration under ultrasonication for 2 min, and then vibrated at 298 K for 0–120 min. The adsorbents were separated by a magnet. The concentrations of dyes were analyzed by a UV-4100 spectrophotometer. The initial pH of dye solution was adjusted at different values with HCl or NaOH aqueous solution [22].

2.5. Desorption experiments

Desorption experiments were carried out as previously described, with a minor modification [23]. The magnetic material containing dyes was shaken with 10 mL of a mixture of anhydrous ethanol and NaOH (0.01 mol L⁻¹) solution at 298 K for 20 min, with the content of NaOH solution being 10% (V/V). Subsequently, the adsorbent was magnetically separated. This process was repeated three times. Finally, the adsorbent was washed with deionized water and anhydrous ethanol to remove the excess NaOH.

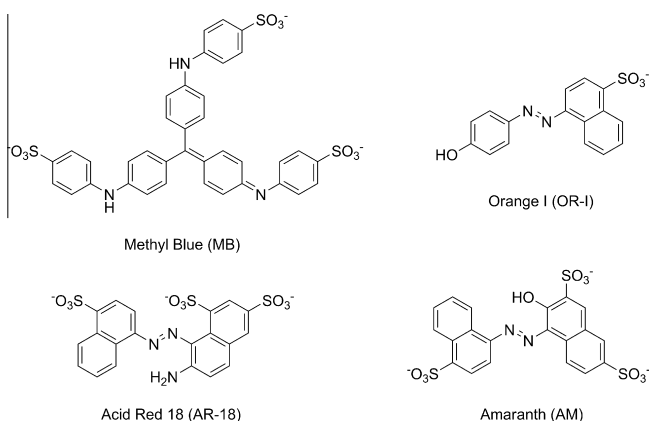


Fig. 1. Structures of MB, OR-I, AM and AR-18.

3. Results and discussion

3.1. Characterization of the adsorbents

The TEM image of the $\text{Fe}_3\text{O}_4@\text{GPTMS@P-Lys}$ MNPs is shown in Fig. 2, which reveals that the diameter of the MNPs is around 10 nm, with a generally homogeneous size.

The FT-IR spectra of the Fe_3O_4 -MNPs (Fig. 3) identify that the magnetic nanoparticles were modified with poly-lysine. Characteristic bands from the Fe–O stretching vibrations are observed at $450\text{--}750\text{ cm}^{-1}$ (Fig. 3a) [24]. The Fe_3O_4 cross-linked with GPTMS is confirmed by bands at 902 cm^{-1} and 1098 cm^{-1} which are assigned to the Si–O group, the C–H bands of propyl are recognized at 2860 and 2922 cm^{-1} , and characteristic peak of epoxide group at 1196 cm^{-1} (Fig. 3b) [25,26]. Fig. 3c displays that the characteristic peak of epoxide group disappears at 1196 cm^{-1} and a wider band can be seen at $3300\text{--}3450\text{ cm}^{-1}$ as a result of some free $-\text{NH}_2$ groups in poly-lysine. Therefore, compared with two spectra in Fig. 3b and c, the modification of the $\text{Fe}_3\text{O}_4@\text{GPTMS@P-Lys}$ is validated. Additionally, the percentage of weight lost in the TGA curve (Fig. S1, ESI) further suggests the modified results.

The superparamagnetic properties are confirmed by the room-temperature magnetization curves, because remanence and coercivity neither appeared [19,27]. The saturation magnetization of Fe_3O_4 , $\text{Fe}_3\text{O}_4@\text{GPTMS}$ and $\text{Fe}_3\text{O}_4@\text{GPTMS@P-Lys}$ MNPs is 51, 47 and 35 emu g^{-1} , respectively (Fig. S2, ESI). The crystals of the three MNPs are cubic spine structures, which can be observed at XRD patterns (Fig. S3, ESI) [28]. The structure of Fe_3O_4 was further confirmed by XPS (Fig. S4, ESI) [29]. The BET surface area of $\text{Fe}_3\text{O}_4@\text{GPTMS@P-Lys}$ MNPs is $119.22\text{ m}^2\text{ g}^{-1}$, and the average pore size (129.30 \AA) was calculated from the desorption isotherms with a BJH model (Fig. S5, ESI).

3.2. Adsorption properties of the MNPs for anionic dyes

3.2.1. Effects of pH on adsorption and the adsorption mechanism

pH is a very crucial parameter that affects the adsorption efficiency of anionic dyes. The effects of pH on the adsorption of anionic dyes were studied over the pH ranges $1.0\text{--}13.0$ [15,30]. The adsorption quantity climbed as the decrease of the original pH of the solution from 4.0 to 1.0 (Fig. 4). The adsorption mechanism can be explained by the protonation of amino groups. In acid condition, the amino groups of $\text{Fe}_3\text{O}_4@\text{GPTMS@Plys}$ were protonated to possess positive charges, which could be observed from the pH-dependent zeta potential (point of zero charge, pH 4.8) of $\text{Fe}_3\text{O}_4@\text{GPTMS@Plys}$ (Fig. S6, ESI). The amino cations of modified MNPs could interact with sulfonate anions of anionic dye by electrostatic adsorption. Although adsorption quantity continued increasing at $\text{pH} < 2.0$, the initial pH 2.0 was selected to investigate the adsorption of anionic dyes because lower pH could accelerate the decomposition of the adsorbent [12].

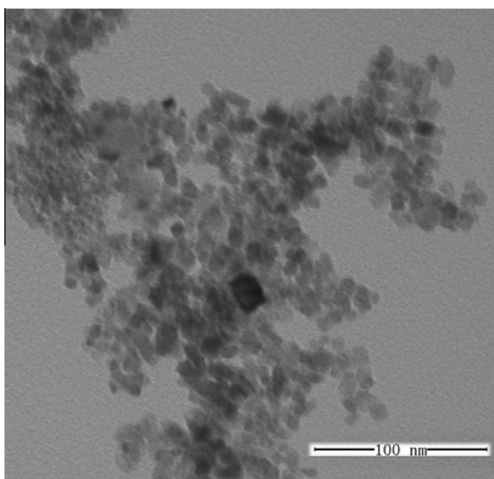


Fig. 2. TEM image of $\text{Fe}_3\text{O}_4@\text{GPTMS@P-Lys}$ MNPs.

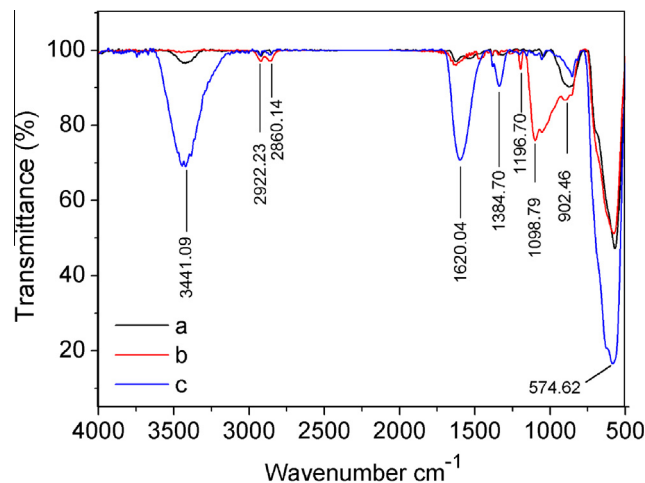


Fig. 3. FT-IR spectra of MNPs. (a) Fe_3O_4 , (b) $\text{Fe}_3\text{O}_4@\text{GPTMS}$ and (c) $\text{Fe}_3\text{O}_4@\text{GPTMS@P-Lys}$.

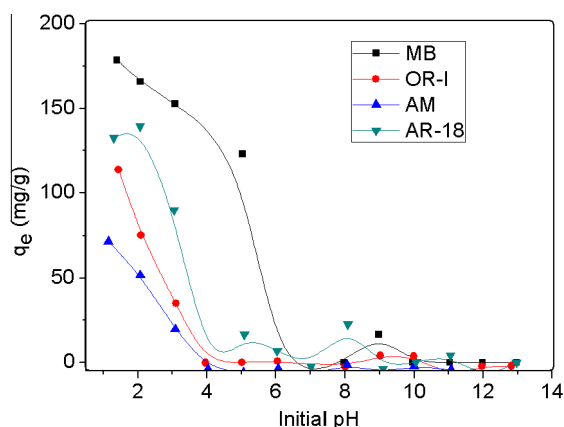


Fig. 4. Effects of pH on adsorption of anionic dyes by $\text{Fe}_3\text{O}_4@\text{GPTMS@P-Lys}$. Adsorbent, 1.00 g L^{-1} ; organic dye, 200 mg L^{-1} ; time, 60 min; temperature, 298 K .

$\text{O}_4@\text{GPTMS@Plys}$ (Fig. S6, ESI). The amino cations of modified MNPs could interact with sulfonate anions of anionic dye by electrostatic adsorption. Although adsorption quantity continued increasing at $\text{pH} < 2.0$, the initial pH 2.0 was selected to investigate the adsorption of anionic dyes because lower pH could accelerate the decomposition of the adsorbent [12].

Fig. 4 shows that the adsorption quantity of AR-18, OR-I, MB and AM is 140 , 75 , 165 and 50 mg g^{-1} at pH 2.0 , respectively. The adsorption quantity of $\text{Fe}_3\text{O}_4@\text{GPTMS@P-Lys}$ for anionic dyes is much higher than that of $\text{Fe}_3\text{O}_4@\text{GPTMS@Gly}$ (the value for AR-18, OR-I and MB is 40 , 55 and 120 mg g^{-1} , respectively) [14] and $\text{Fe}_3\text{O}_4@\text{GPTMS@Lys}$ (the value for AR-18, OR-I and MB is 70 , 75 and 130 mg g^{-1} , respectively) [15]. The reasonable explanations for these results are that the amino groups of the adsorbent are protonated at low pH to form amino cations and polylysine contains much more amino groups than lysine and glycine (Fig. 5). These protonated amino groups result in the adsorbent possessing positive charges which can interact with the sulfonate anions of anionic dye through electrostatic adsorption. Therefore, the adsorbent can adsorb anionic dyes at low pH and the adsorption capacity of $\text{Fe}_3\text{O}_4@\text{GPTMS@P-Lys}$ for anionic dyes is higher.

3.2.2. Adsorption kinetics

Fig. 6 illustrates the effects of contact time on the adsorption for the anionic dyes. The data show that the adsorbent is available for

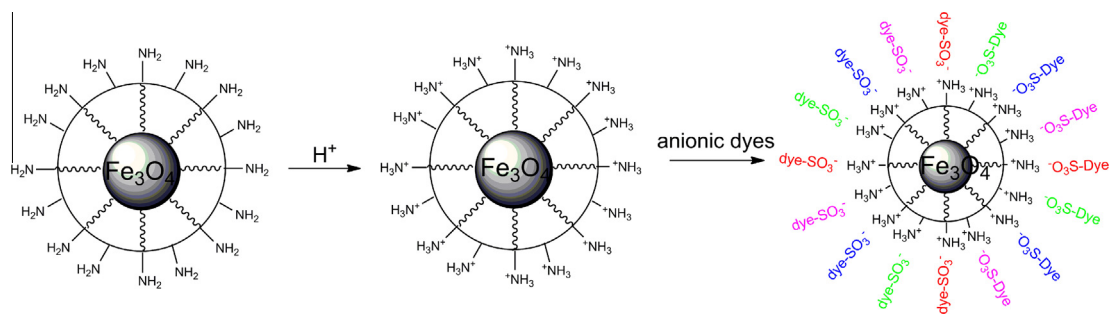


Fig. 5. Proposed mechanism for the adsorption of anionic dyes by $\text{Fe}_3\text{O}_4@\text{GPTMS}@P\text{-Lys}$.

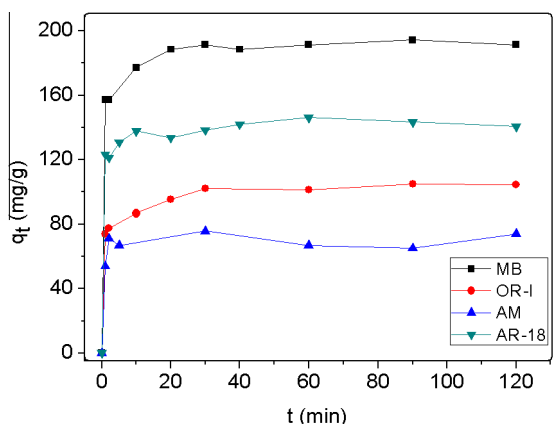


Fig. 6. Effects of time on adsorption of MB, OR-I, AM, AR-18 by $\text{Fe}_3\text{O}_4@\text{GPTMS}@P\text{-Lys}$. Adsorbent, 1.00 g L^{-1} ; anionic dye, 200 mg L^{-1} ; pH, 2.0; time, 0–120 min; temperature, 298 K.

the four dyes, and the reaction reaches the adsorption equilibrium after about 40 min, but keeping on extending contact time is inessential for the removal of the dyes. The larger surface areas and the electrostatic interaction can account for the fine adsorption capacity.

It is essential to found well defined kinetic models so as to seek out the rate-controlling step of the adsorption process [31]. Several adsorption kinetic models have been founded to understand the adsorption kinetics and the rate-limiting step. The pseudo-first-order, pseudo-second-order and intraparticle diffusion models are the noted models to research the adsorption kinetics and quantify the extent of uptake in adsorption kinetics [32]. Accordingly, in this work, we studied the adsorption kinetics by dint of the three models (Eqs. (1)–(3)).

Pseudo-first-order:

$$\ln(q_e - q_t) = \ln q_e - k_1 t \quad (1)$$

Pseudo-second-order:

$$t/q_t = 1/k_2 q_e^2 + t/q_e \quad (2)$$

Intraparticle diffusion:

$$q_t = k_3 t^{1/2} \quad (3)$$

where q_e and q_t (mg g^{-1}) are the amounts of dyes in the adsorption equilibrium and at time t (min); and k_1 (min^{-1}), k_2 ($\text{g mg}^{-1} \text{min}^{-1}$) and k_3 ($\text{mg g}^{-1} \text{min}^{-1/2}$) are the kinetic rate constants for the pseudo-first-order, pseudo-second-order and intraparticle diffusion models. The kinetic adsorption data were adapted to Eqs. (1)–(3), and the calculated results are displayed in Table 1. According to the correlation coefficients, the experimental data fit to the pseudo-second-order model better than other models (Fig. S7, ESI), thus, the rate-limiting step might be the chemical adsorption [22,33,34].

3.2.3. Adsorption isotherms

The adsorption isotherm plays a significant role in evaluating the adsorption properties of $\text{Fe}_3\text{O}_4@\text{GPTMS}@P\text{-Lys}$ MNPs [35]. To depict the adsorption process thoroughly, three well-known isotherm equations, Langmuir, Freundlich and Temkin (Eqs. (4)–(6)), were applied [36].

Langmuir equation:

$$C_e/q_e = C_e/q_m + 1/K_L q_m \quad (4)$$

where q_e (mg g^{-1}) is the equilibrium adsorption capacity of dye on the adsorbent; C_e (mg L^{-1}) is the equilibrium dye concentration in solution; q_m (mg g^{-1}), the maximum capacity of the adsorbent; and K_L (L mg^{-1}), the Langmuir constant.

Freundlich equation:

$$q_e = K_F C_e^{1/n} \quad (5)$$

where q_e and C_e are defined as above; K_F (L mg^{-1}) is the Freundlich constant; and n is the heterogeneity factor.

Temkin equation:

$$q_e = A + B \ln C_e \quad (6)$$

where q_e and C_e are defined as above; A and B are constants.

The adsorption isotherms are shown in Fig. 7. The experimental data indicate that the equilibrium adsorption capacity of the dye is direct proportional to the initial dye concentration. The adsorption reaction fits in with the Langmuir better than others according to the correlation coefficients (Fig. S8, ESI). The result

Table 1
Parameter values of the kinetics models fitting to the experimental results in Fig. 5 for organic dyes.

Organic dyes	q (mg g^{-1}) ^a	1st order			2nd order			Intraparticle diffusion model	
		R^2	k_1	q_e (mg g^{-1})	R^2	k_2	q_e (mg g^{-1})	R^2	k_3
MB	193.9759	0.43485	0.02799	187.23	0.99984	0.01038	193.17651	0.90438	41.6862
OR-I	104.35897	0.64637	0.05135	104.14	0.99958	0.00710	103.19854	0.95773	22.2822
AM	84.04255	0.06141	0.00693	47.45	0.99121	0.01687	83.55160	0.1524	17.2595
AR-18	134.69388	0.53335	0.17257	134.69	0.99946	0.02439	134.35306	0.83406	33.2681

^a Experimental data of adsorption capacities.

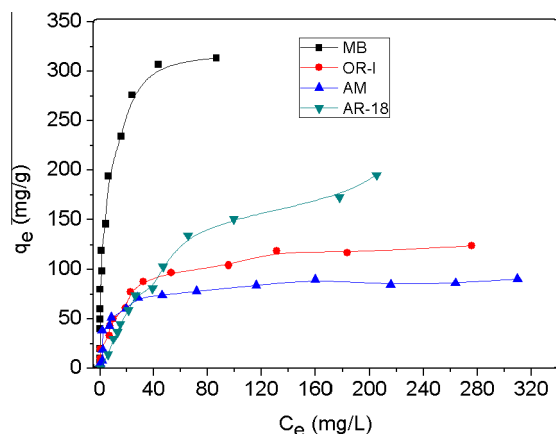


Fig. 7. Equilibrium isotherms of organic dyes by $\text{Fe}_3\text{O}_4\text{@GPTMS@P-Lys}$ performed in bath mode. Adsorbent, 1.00 g L^{-1} ; anionic dyes, $20\text{--}400 \text{ mg L}^{-1}$; temperature, 298 K ; time: 60 min.

demonstrated the lysine groups on the surface determined the adsorption ability, which was consistent with the adsorption mechanism. The maximum adsorption capacities (q_m) for the dyes were worked out by the Langmuir equation and are listed in Table 2. The Langmuir maximum quantity (q_m) for four dyes: MB, OR-I, AM and AR-18 is 318 , 128 , 90 and 245 mg g^{-1} , respectively. In particular, the q_m of the adsorbent for anionic dyes is much higher than that of $\text{Fe}_3\text{O}_4\text{@GPTMS@Lys}$ (MB: 185 mg g^{-1} , OR-I: 71 mg g^{-1} , AR-18: 83 mg g^{-1}) [15], which conforms to the original intention of $\text{Fe}_3\text{O}_4\text{@GPTMS@P-Lys}$ MNPs. Besides, the q_m of the adsorbent for MB, OR-I and AR-18 is over 125 mg g^{-1} , which is higher than that for traditional adsorbents reported in literature (Table 3). Additionally, $\text{Fe}_3\text{O}_4\text{@GPTMS@P-Lys}$ MNPs surpass other adsorbents in the field of effortless separation, high adsorption capacities, producing little environmental pollution and reusability.

3.2.4. Recycle of the adsorbent

The data in Fig. 4 illustrate that the adsorbent can favorably adsorb anionic dyes at $\text{pH} < 4.0$, therefore, we can also indicate that the adsorbed organic dyes released in solution by adjusting pH [40]. In practice, to improve desorption efficiency, desorption experiments were carried out with a mixture solution of ethanol and NaOH because organic dyes dissolved readily in organic solvents. According to Fig. 8 after three cycles, MB and AR-18 have gained about 90% of adsorption efficiency, meanwhile, the other organic dyes OR-I and AM is around 80%. However, the adsorption efficiency of the last two dyes is lower than others after three cycles, the equilibrium adsorption capacity of OR-I and AM still reaches 102 , 80 mg g^{-1} , respectively. Consequently, the adsorbent can be efficiently reused to remove anionic dyes from aqueous solution.

Table 2

Langmuir, Freundlich and Temkin adsorption isotherm constant, correlation coefficient and q_m .

Organic dyes	Langmuir			Freundlich			Temkin
	K_L (L mg^{-1})	q_m (mg g^{-1})	R^2	K_F ($\text{mg}^{1-(1/n)} \text{L}^{1/n} \text{g}^{-1}$)	n	R^2	R^2
MB	0.44921	318.47	0.9936	109.169	3.805	0.9089	0.9367
OR-I	0.07335	128.20	0.9950	29.160	3.270	0.8883	0.9131
AM	0.12208	90.82	0.9974	10.712	2.366	0.7602	0.9023
AR-18	0.01624	245.09	0.9881	6.358	1.464	0.9309	0.9769

Table 3

Comparison of maximum adsorption capacity of various adsorbents for MB.

Adsorbents	q_m (mg g^{-1})/MB	Refs.
Organo-bentonite	98.15	[37]
PET carbon	33.4	[38]
Saw dust-pitch pine	27.78	[39]
$\text{Fe}_3\text{O}_4\text{@GPTMS@Lys}$	185	[15]
$\text{Fe}_3\text{O}_4\text{@GPTMS@P-Lys}$	318	This work

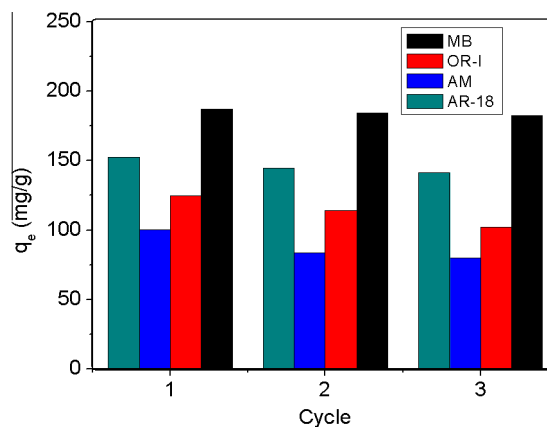


Fig. 8. Reusability of $\text{Fe}_3\text{O}_4\text{@GPTMS@P-Lys}$ for 3 cycles. Adsorbent, 1.00 g L^{-1} ; anionic dyes, 200 mg L^{-1} ; temperature, 298 K ; pH , 2.0; time: 60 min.

4. Conclusions

Novel Fe_3O_4 magnetic nanoparticles were synthesized by low toxic 3-glycidoxypropyltrimethoxysilane and poly-lysine. The maximum adsorption capacities of the $\text{Fe}_3\text{O}_4\text{@GPTMS@P-Lys}$ MNPs for anionic dyes from aqueous solution enhanced because poly-lysine has even more amino groups. The adsorption kinetics is consistent with the pseudo-second-order model and the adsorption isotherms fits to the Langmuir. Moreover, the adsorbent can be reused in suitable condition. In the light of effortless separation, high adsorption capacities, producing little environmental pollution and reusability, the magnetic nanoparticles may play an important role in wastewater treatment in the future.

Acknowledgment

This study was supported by the National Basic Research Program of China (2010CB933504).

Appendix A. Supplementary data

Supplementary data associated with this article can be found, in the online version, at <http://dx.doi.org/10.1016/j.cej.2014.09.094>.

References

- [1] R. Rahimi, H. Kerdari, M. Rabbani, M. Shafiee, Synthesis, characterization and adsorbing properties of hollow Zn-Fe₂O₄ nanospheres on removal of Congo red from aqueous solution, *Desalination* 280 (2011) 412–418.
- [2] W. Konicki, D. Sibera, E. Mijowska, Z. Lendzion-Bieluń, U. Narkiewicz, Equilibrium and kinetic studies on acid dye Acid Red 88 adsorption by magnetic ZnFe₂O₄ spinel ferrite nanoparticles, *J. Colloid Interface Sci.* 398 (2013) 152–160.
- [3] G.M. Walker, L. Hansen, J.A. Hanna, S.J. Allen, Kinetics of a reactive dye adsorption onto dolomitic sorbents, *Water Res.* 37 (2003) 2081–2089.
- [4] S. Sekar, M. Surianarayanan, V. Ranganathan, D.R. MacFarlane, A.B. Mandal, Choline-based ionic liquids-enhanced biodegradation of azo dyes, *Environ. Sci. Technol.* 46 (2012) 4902–4908.
- [5] T. Soltani, M.H. Entezari, Sono-synthesis of bismuth ferrite nanoparticles with high photocatalytic activity in degradation of Rhodamine B under solar light irradiation, *Chem. Eng. J.* 223 (2013) 145–154.
- [6] G.M. Walker, L.R. Weatherley, Adsorption of acid dyes on to granular activated carbon in fixed beds, *Water Res.* 31 (1997) 2093–2101.
- [7] B.K. Nandi, A. Goswami, M.K. Purkait, Removal of cationic dyes from aqueous solutions by kaolin: kinetic and equilibrium studies, *Appl. Clay Sci.* 42 (2009) 583–590.
- [8] C.A.P. Almeida, N.A. Debacher, A.J. Downs, L. Cottet, C.A.D. Mello, Removal of methylene blue from colored effluents by adsorption on montmorillonite clay, *J. Colloid Interface Sci.* 332 (2009) 46–53.
- [9] C. Namasivayam, R.T. Yamuna, D. Aras, Removal of procion orange from wastewater by adsorption on waste red mud, *Sep. Purif. Technol.* 37 (2002) 2421–2431.
- [10] G. McKay, M.S. Otterburn, J.A. Aga, Fullers earth and fired clay as adsorbents for dyestuffs – equilibrium and rate studies, *Water Air Soil Pollut.* 24 (1985) 307–322.
- [11] Z.Y. Zhang, J.L. Kong, Novel magnetic Fe₃O₄@C nanoparticles as adsorbents for removal of organic dyes from aqueous solution, *J. Hazard. Mater.* 193 (2011) 325–329.
- [12] F. Ge, H. Ye, M.M. Li, B.X. Zhao, Efficient removal of cationic dyes from aqueous solution by polymer-modified magnetic nanoparticles, *Chem. Eng. J.* 198–199 (2012) 11–17.
- [13] D.P. Li, Y.R. Zhang, X.X. Zhao, B.X. Zhao, Magnetic nanoparticles coated by aminoguanidine for selective adsorption of acid dyes from aqueous solution, *Chem. Eng. J.* 232 (2013) 425–433.
- [14] Y.R. Zhang, S.Q. Wang, S.L. Shen, B.X. Zhao, A novel water treatment magnetic nanomaterial for removal of anionic and cationic dyes under severe condition, *Chem. Eng. J.* 233 (2013) 258–264.
- [15] Y.R. Zhang, S.L. Shen, S.Q. Wang, J. Huang, P. Su, Q.R. Wang, B.X. Zhao, A dual function magnetic nanomaterial modified with lysine for removal of organic dyes from water solution, *Chem. Eng. J.* 239 (2014) 250–256.
- [16] L. Hua, Y.M. Huang, Q.W. Chen, Fe_xCo_{3-x}O₄ nanoporous particles stemmed from metal-organic frameworks Fe₃[Co(CN)₆]₂: a highly efficient material for removal of organic dyes from water, *J. Alloy. Compd.* 559 (2013) 57–63.
- [17] Z.F. Wang, H.S. Guo, Y.L. Yu, N.Y. He, Synthesis and characterization of novel magnetic carrier with its composition of Fe₃O₄/carbon using hydrothermal reaction, *J. Magn. Magn. Mater.* 302 (2006) 397–404.
- [18] X.L. Zhao, Y.L. Shi, T. Wang, Y.Q. Cai, G.B. Jiang, Preparation of silica-magnetite nanoparticle mixed hemimicelle sorbents for extraction of several typical phenolic compounds from environmental water samples, *J. Chromatogr. A* 1188 (2008) 140–147.
- [19] Y. Zhou, S.X. Wang, B.J. Ding, Z.M. Yang, Modification of magnetite nanoparticles via surface-initiated atom transfer radical polymerization (ATRP), *Chem. Eng. J.* 138 (2008) 578–585.
- [20] F. Ge, M.M. Li, H. Ye, B.X. Zhao, Effective removal of heavy metal ions Cd²⁺, Zn²⁺, Pb²⁺, Cu²⁺ from aqueous solution by polymer-modified magnetic nanoparticles, *J. Hazard. Mater.* 211–212 (2012) 366–372.
- [21] X. Zhao, J. Wang, F. Wu, T. Wang, Y. Cai, Removal of fluoride from aqueous media by Fe₃O₄@Al(OH)₃ magnetic nanoparticles, *J. Hazard. Mater.* 173 (2010) 102–109.
- [22] L.R. Luo, K. Shen, Q.Y. Xu, Q. Zhou, W. Wei, M.A. Gondal, Preparation of multiferroic Co substituted BiFeO₃ with enhanced coercive force and its application in sorption removal of dye molecules from aqueous solution, *J. Alloy. Compd.* 558 (2013) 73–76.
- [23] A. Debrassi, A.F. Correa, T. Baccarin, N. Nedelko, A. Ślowska-Waniewsk, K. Sobczak, P. Dłużewski, J.M. Greneche, C.A. Rodrigues, Removal of cationic dyes from aqueous solutions using N-benzyl-O-carboxymethylchitosan magnetic nanoparticles, *Chem. Eng. J.* 183 (2012) 284–293.
- [24] G.Y. Li, K.L. Huang, Y.R. Jiang, P. Ding, D.L. Yang, Preparation and characterization of carboxyl functionalization of chitosan derivative magnetic nanoparticles, *Biochem. Eng. J.* 40 (2008) 408–414.
- [25] R.T. Olsson, M.S. Hedenqvist, V. Strom, J. Deng, S.J. Savage, U.W. Gedde, Core-shell structured ferrite-silsesquioxane-epoxy nanocomposites: composite homogeneity and mechanical and magnetic properties, *Polym. Eng. Sci.* (2011) 862–874.
- [26] P.C. Sahoo, Y.N. Jang, S.W. Lee, Immobilization of carbonic anhydrase and an artificial Zn(II) complex on a magnetic support for biomimetic carbon dioxide sequestration, *J. Mol. Catal. B Enzym.* 82 (2012) 37–45.
- [27] H.O. Qu, H. Ma, W.L. Zhou, C.J. O'Connor, In situ surface functionalization of magnetic nanoparticles with hydrophilic natural amino acids, *Inorg. Chim. Acta* 389 (2012) 60–65.
- [28] L.M. Zhou, J.P. Xu, X.Z. Liang, Z.R. Liu, Adsorption of platinum (IV) and palladium (II) from aqueous solution by magnetic cross-linking chitosan nanoparticles modified with ethylenediamine, *J. Hazard. Mater.* 182 (2010) 518–524.
- [29] J. Lu, X.L. Jiao, D.R. Chen, W. Li, Solvothermal synthesis and characterization of Fe₃O₄ and γ-Fe₂O₃ nanoplates, *J. Phys. Chem. C* 113 (2009) 4012–4017.
- [30] L.H. Ai, L.L. Li, Efficient removal of organic dyes from aqueous solution with ecofriendly biomass-derived carbon@montmorillonite nanocomposites by one-step hydrothermal process, *Chem. Eng. J.* 223 (2013) 688–695.
- [31] S.R. Shirsath, A.P. Patil, R. Patil, J.B. Naik, P.R. Gogate, S.H. Sonawane, Removal of Brilliant Green from wastewater using conventional and ultrasonically prepared poly (acrylic acid) hydrogel loaded with kaolin clay: a comparative study, *Ultrason. Sonochem.* 20 (2013) 914–923.
- [32] T. Madrakian, A. Afkhami, M. Ahmadi, Adsorption and kinetic studies of seven different organic dyes onto magnetite nanoparticles loaded tea waste and removal of them from wastewater samples, *Spectrochim. Acta A* 99 (2012) 102–109.
- [33] L.L. Fan, Y. Zhang, C.N. Luo, F.G. Lu, H.M. Qiu, M. Sun, Synthesis and characterization of magnetic β-cyclodextrin-chitosan nanoparticles as nanoadsorbents for removal of methyl blue, *Int. J. Biol. Macromol.* 50 (2012) 444–450.
- [34] Q. Yu, R.Q. Zhang, S.B. Deng, J. Huang, G. Yu, Sorption of perfluorooctane sulfonate and perfluorooctanoate on activated carbons and resin: kinetic and isotherm study, *Water Res.* 43 (2009) 1150–1158.
- [35] F. Liu, Y.J. Jin, H.B. Liao, L. Cai, M.P. Tong, Y.L. Hou, Facile self-assembly synthesis of titanate/Fe₃O₄ nanocomposites for the efficient removal of Pb²⁺ from aqueous systems, *J. Mater. Chem. A* 1 (2013) 805–813.
- [36] S. Qadri, A. Ganoe, Y. Haik, Removal and recovery of acridine orange from solutions by use of magnetic nanoparticles, *J. Hazard. Mater.* 169 (2009) 318–323.
- [37] X.L. Hao, H. Liu, G.S. Zhang, H. Zou, Y.B. Zhang, M.M. Zhou, Y.C. Gu, Magnetic field assisted adsorption of methyl blue onto organo-bentonite, *Appl. Clay Sci.* 55 (2012) 177–180.
- [38] F.S. Zhang, H. Itoh, Adsorbents made from waste ashes and post-consumer PET and their potential utilization in wastewater treatment, *J. Hazard. Mater.* 101 (2003) 323–337.
- [39] F. Ferrero, Dye removal by low cost adsorbents: hazelnut shells in comparison with wood sawdust, *J. Hazard. Mater.* 142 (2007) 144–152.
- [40] Y.F. Lin, H.W. Chen, P.S. Chien, Application of bifunctional magnetic adsorbent to adsorb metal cations and anionic dyes in aqueous solution, *J. Hazard. Mater.* 185 (2011) 1124–1130.